

This is a repository copy of *The use of reverberation chambers in the quantitative assessment of the risk associated with the installation of electronic systems on vehicles.*

White Rose Research Online URL for this paper:
<https://eprints.whiterose.ac.uk/133875/>

Version: Accepted Version

Conference or Workshop Item:

Marvin, A C orcid.org/0000-0003-2590-5335, Konefal, T, Dawson, J F orcid.org/0000-0003-4537-9977 et al. (1 more author) (2007) The use of reverberation chambers in the quantitative assessment of the risk associated with the installation of electronic systems on vehicles. In: EMC Europe Workshop 2007, 14-15 Jun 2007.

Reuse

Items deposited in White Rose Research Online are protected by copyright, with all rights reserved unless indicated otherwise. They may be downloaded and/or printed for private study, or other acts as permitted by national copyright laws. The publisher or other rights holders may allow further reproduction and re-use of the full text version. This is indicated by the licence information on the White Rose Research Online record for the item.

Takedown

If you consider content in White Rose Research Online to be in breach of UK law, please notify us by emailing eprints@whiterose.ac.uk including the URL of the record and the reason for the withdrawal request.

THE USE OF REVERBERATION CHAMBERS IN THE QUANTITATIVE ASSESSMENT OF THE RISK ASSOCIATED WITH INSTALLATION OF ELECTRONIC SYSTEMS ON VEHICLES

A C Marvin, T Konefal, J F Dawson, and M P Robinson

Department of Electronics, University of York

Heslington, York YO10 5DD, England

E-mail: acm@ohm.york.ac.uk

Abstract: The paper describes the use of reverberation chamber measurements to verify the probability of failure of a vehicle parking sensor corresponds with the theoretical log-normal pdf predicted for current coupled into cables in a reverberant environment. This provides the basis for a quantitative risk assessment system for vehicle electronics.

I. INTRODUCTION

The EU SAFETEL Project was concerned with the safety implications of installing electronic equipment on vehicles. Part of the project concerned the development of a risk assessment model suitable for predicting an upper bound on the probability of failure of an electronic system installed inside a vehicle that is irradiated externally or internally. Only limited information on the immunity of the device and associated cabling is required. As an example, the model is used to demonstrate the probability of failure of a system due to irradiation from Digital Audio Broadcast (DAB) transmitters in the United Kingdom (UK). The failure probability is found to be highly sensitive to the clearance above the vehicle chassis of wire looms attached to the system, and to the accuracy with which the electric field is measured during an immunity test for the system/cable combination. The failure probability predicted by the risk assessment model is consistent with common observations of a log-normal distribution in the terminating power of receiving cables inside an irradiated vehicle confirmed by measurements in a reverberation chamber.

In this paper we describe the experiments undertaken in the reverberation chamber and present the results of the experiments which illustrate their correspondence with the theoretical and observed statistics of the power received by cable terminations in a lossy enclosed space such as a vehicle. The rotational positions of the stirrer substitute for the statistical nature of the excitation fields in the vehicle and the variations of positioning of the cables within the vehicle. An example system comprising a multi-sensor ultrasonic parking warning system was used in the

experiments and good agreement was achieved between the predictions and the observed failures of the system when under test.

II. IMMUNITY PROFILE OF EUT

The major route by which EMI will enter a subsystem is likely to be via cabling. Therefore method used here to measure the immunity profile for a vehicular subsystem is by means of bulk current injection onto a sensor cable. The particular subsystem examined is an ultrasonic parking unit. This device has 8 ultrasonic sensors (four on the front bumper of the car and four on the rear bumper), and a digital display of the distance to a potential hazard when parking. The display and ultrasonic sensors are connected to a central processing unit (CPU) plastic 'black box.' The ultrasonic sensors are connected to the CPU by rather long cables which would normally be positioned against the metal chassis of the car, thus forming a circular wire/ground plane transmission line.

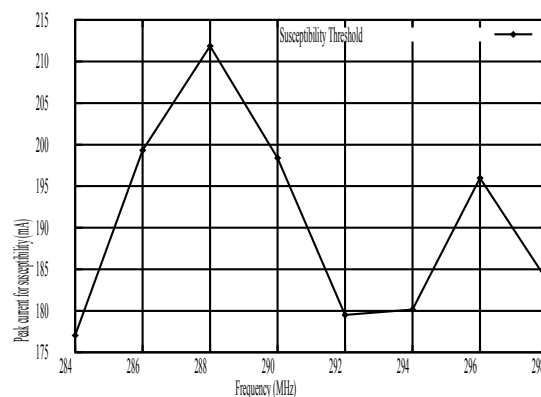


Fig.1. Current susceptibility profile for parking sensor in range 284MHz-298MHz

The mode of failure of the parking sensor in the frequency range 284MHz-298MHz as the current level was increased followed a consistent pattern. The digital back lit LCD display would first become

erratic, with varying and inaccurate numbers being displayed. The display would then freeze, and after or second or so would completely disappear, with even the back illuminating light being extinguished.

III. STATISTICAL TREATMENT OF FIELD COUPLING

With a knowledge of the susceptibility threshold of a device at the end of a cable, which for example may have been obtained using a Bulk Current Injection (BCI) immunity test, the signal picked up by a cable attached to the device within a vehicle can be simulated using full wave numerical electromagnetic solvers. By comparing the level of signal induced in the cable with the measured immunity threshold, it can be determined whether or not the device at the end of the cable will fail.

This deterministic approach is inadequate for two reasons. Firstly, the traditional numerical methods are computationally intensive. Even with modern computers with clock speeds of 2-3 GHz, the methods will generally take several hours to simulate the signals picked up by a single transmission line of a given geometry inside an irradiated vehicle. A statistical analysis involving variations of cable length and position is thus not feasible using these methods. We note however that some progress has been made using the Intermediate Level Circuit Modelling or ILCM technique [1]. Using the ILCM technique, a deterministic solution to such a problem can generally be found in seconds, typically three to four orders of magnitude faster than traditional numerical techniques. Secondly, the actual threat signal induced on a cable or wire loom inside a vehicle due to an EM emission, either from within the vehicle or from the vehicle exterior, is a poorly posed deterministic problem. It is well known that even very small changes in the position of the transmitter or receiving wire loom, and indeed any other sizeable objects within the vehicle, can alter the signal picked up by the wire loom significantly. Instead, the signal picked up by the wire loom, regarded as a transmission line, can be treated in a statistical manner. For example, it is reported [2] that the probability density function (PDF) of the power induced in representative cables typically follows a log-normal distribution as the cable position is varied, with a typical standard deviation in the range 3-6dB. Such behaviour has been replicated using the ILCM technique. In particular, the upper tail end of the power distribution is found to follow a log-normal distribution. This is significant from the point of view of risk assessment since it is the upper tail of the distribution that determines the probability of failure when the latter is relatively low.

The interior of a vehicle is a reverberant environment. The power received by a dipole in an ideal reverberation chamber (RC) is found to follow an exponential distribution (i.e. a chi-square distribution with two degrees of freedom), providing the chamber has sufficient losses to allow significant excitation of a sufficient number of modes (10-30) [3,4]. This is true

whether the observation point is fixed and the frequency is varied or the frequency is fixed and the point of observation is varied. This is also true for a mode stirred/tuned reverberation chamber where the stirrer angle is the varied parameter. Providing that conditions such as unequal shielding of regions, sub enclosures,, closely spaced walls that could act as waveguides below cut-off, or significant direct illumination of the dipole by the source do not apply, it would normally be expected that received power would have an exponential distribution. This in fact corresponds to a Rayleigh distribution in the modulus of the voltage received by a dipole antenna. When any anisotropy is introduced however, the received antenna power distribution usually resembles a log-normal distribution [2]. The fact that a cable held up against a vehicle wall in a general sense resembles an anisotropic configuration for a dipole, and the fact that for such a cable we usually obtain cable terminal power statistics that are log-normal in nature, raises the analogy between an irradiated vehicle and a reverberation chamber. Certainly a vehicle is a large metal enclosure, of approximately rectangular geometry, that will be electrically large at many of the frequencies of interest for EMC purposes, typically from tens of MHz upwards.

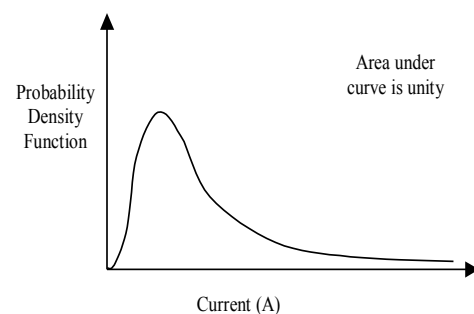


Fig. 2. Statistical distribution of current entering the vehicle subsystem.

We have shown [5] elsewhere that the field behaviour in a vehicle, loaded with contents, passengers etc. can behave like a reverberation chamber. The final step in defining a probabilistic safety margin comes from combining the measurement of the immunity profile in Figure 1 with the statistical treatment of field ingress/distribution. Figures 2 and 3 illustrate the principles involved. The ideas are based on material presented in [6]. Figure 2 shows an approximate statistical distribution of current at the cable termination near the parking sensor CPU, when the ultrasonic probe cable is installed inside the vehicle (reverberation chamber), and the vehicle is irradiated by a known field. The detailed statistical profile of Figure 2 is determined in Section IV, and the most probable value of current is of course directly proportional to the magnitude of the incident threat field. Figure 3 illustrates how the profile of Figure 2, and the variation of its most probable value with frequency (also calculable from ILCM), can be

combined with a typical immunity profile, for example as measured in Figure 1. It is evident that the probability of malfunction or failure of the vehicle subsystem (parking sensor) is given by the area under the tail of the current statistics profile curve at the point where the curve intersects the immunity profile curve as obtained by measurement using a current injection technique (e.g. BCI).

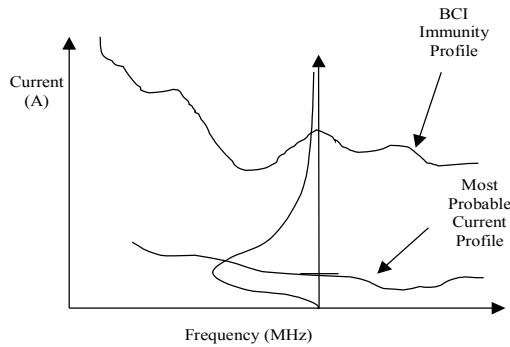


Fig. 3. Use of PDF in Figure 2 together with measured immunity profile of EUT to determine the probability of failure for a given radiated threat level.

As the threat field increases, the most probable current in the statistical current profile of Figure 3 moves proportionally up the ordinate, while the immunity profile remains stationary. Note that at the same time the numerical value of the PDF at its peak will actually decrease, since higher fields are more likely and the area under the PDF curve must remain at unity. The overall result is that a greater area of the tail of the PDF is encapsulated by the point of intersection of the two curves, indicating that the probability of failure has increased. In this way, the probability of failure of the vehicle subsystem or parking sensor may be determined both as a function of frequency and incident threat field level, when the subsystem is installed on the vehicle as intended. Given that the vehicle is being irradiated by a threat signal of known frequency and amplitude, we can obtain the probability of malfunction of a particular vehicle subsystem.

IV. MEASUREMENT OF EUT FAILURE STATISTICS IN A REVERBERATION CHAMBER

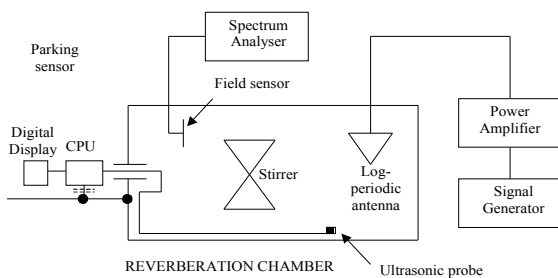


Fig. 4. Experimental set up of parking sensor inside chamber.

The ultrasonic probe cable of length 7.93m is laid out against the floor of the reverberation chamber on a polystyrene spacer of height 2.5cm. The cable is kept at least 30cm away from the vertical chamber walls, to ensure that the distance of the cable from the walls is at least a quarter of a wavelength at 290MHz. The parking sensor exhibits a susceptibility problem at this frequency when the current entering the CPU exceeds about 190mA (-14.4dBA). The ultrasonic probe itself is positioned at one end of the cable, pointing at the ceiling, while the other end of the cable exits the chamber via the centre of a 10cm long copper tube packed with plastic foam material. The relative permittivity of this material is unknown, but is assumed to be close to unity. The other end of the tube leads to the CPU of the parking sensor itself, positioned outside the chamber as in Figure 6. The display and power supply cables are kept outside the chamber to simplify the experiment, preventing any unwanted susceptibility problems from occurring due to EM interference being picked up on the display or power supply cables.

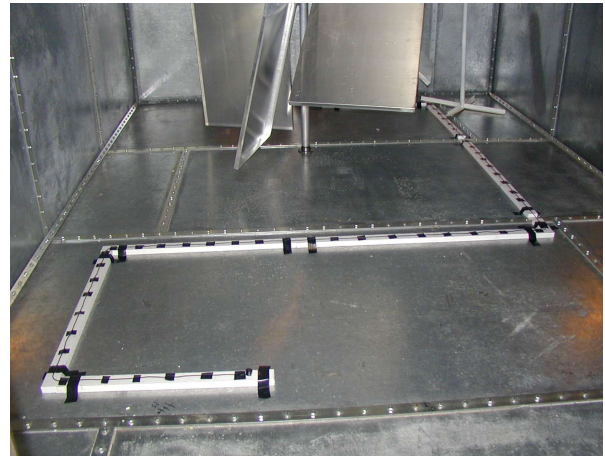


Fig. 5. Layout of the ultrasonic parking sensor cable in the reverberation chamber.



Fig. 6. The exterior of the reverberation chamber, showing the parking sensor CPU, digital display and current probe.

The current entering the CPU outside the chamber is monitored by a current probe. The electric field inside

the chamber was recorded by a calibrated dipole antenna and balun. The Stirrer was rotated in approximately half-degree steps with the field and current recorded for each position.

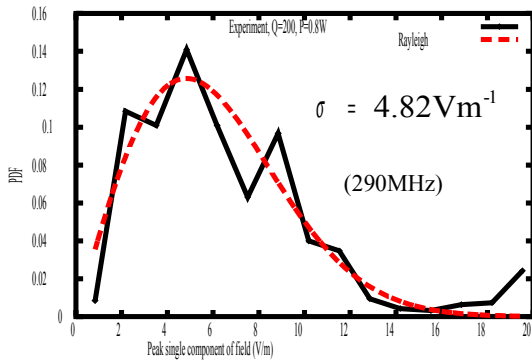


Fig. 7. Field distribution in chamber with absorber.

Figure 7 shows the measured field distribution in the chamber compared with the ideal Rayleigh case. At 290 MHz the reverberation chamber is near its lower usable frequency and must be loaded with absorber to ensure the expected Rayleigh field distribution. Figure 8 shows the measured induced current along with the theoretical log-normal distribution.

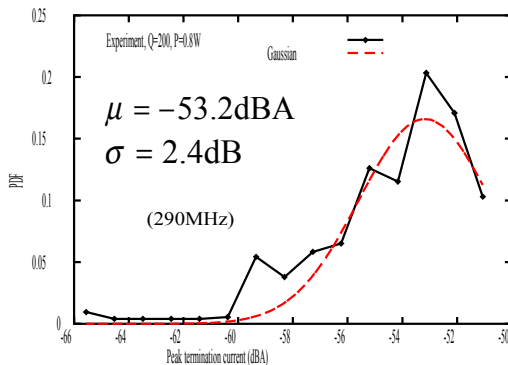


Fig. 8. Experimental distribution of cable termination current I_{Term} for chamber with absorber

In this experiment we were unable to achieve sufficiently high enough field strengths without removing the chamber loading, resulting in the field distribution shown in Figure 9. This corresponds more nearly to the distribution found in cavities with few resonant modes excited.

Figure 10 shows the probability density function of the terminal current entering the CPU of the parking sensor as the stirrer is rotated through 360° . It can be seen that despite the lack of Rayleigh statistics (Figure 9, scaled up by a factor of 7dB), the distribution of terminal current I_{CPU} is still reasonably well modelled by a log-normal distribution. The standard deviation of this distribution is 7.62dB. Also shown in Figure 10 is the current at which the parking sensor was found to fail. This is slightly lower than the value determined by bulk

current injection. The discrepancy is thought to be due to the slightly different terminating conditions of the sensor and the sensor cable.

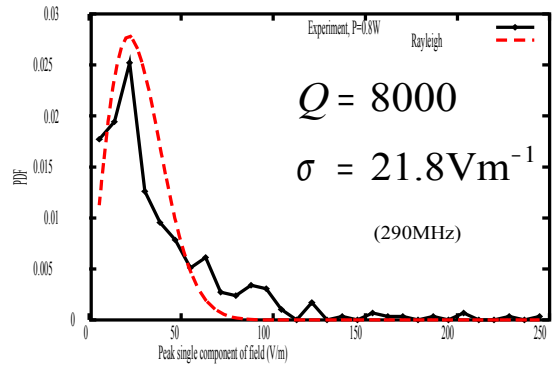


Fig. 9. Field distribution in chamber - no absorber.

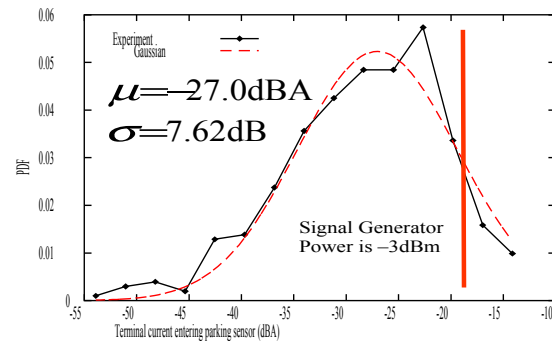


Fig. 10. Distribution of parking sensor terminal current with no absorber in the reverberation chamber.

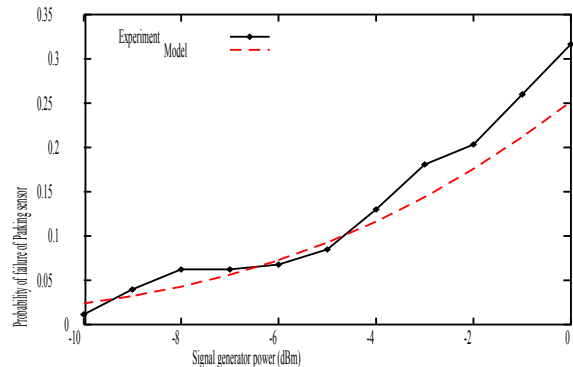


Fig. 11. Experimental and theoretical probability of failure of the parking sensor.

The most probable current I_{CPU} obtained in Figure 10 was $\mu = -27.0 \text{ dBA}$, with a source signal generator power of -3 dBm . Clearly, as the source signal generator power is increased or decreased, the value of μ will rise up and down in proportion. The probability of failure of the parking sensor for a signal generator power of -3 dBm can be found from the area under the curve in Figure 10 that lies to the right of the vertical line at $I_{CPU} = 18.9 \text{ dBA}$. If the signal generator power is reduced by $N \text{ dB}$, the curve in Figure 10 moves to the left by $N \text{ dB}$, and the area under

the curve to the right of the line at $I_{CPU}=18.9\text{dBA}$ decreases. This corresponds to a decreased probability of failure of the parking sensor. In the same way, an increase in the signal generator power of $N\text{dB}$ makes the curve in Figure 10 move to the right by $N\text{dB}$ along the abscissa, and an increased probability of failure is predicted.

With a most probable current of $\mu=-27.0\text{dBA}$ at a source signal generator power of -3dBm , and a threshold for failure of -18.9dBA , the probability of failure of the parking sensor for a signal generator power of $X\text{dBm}$ is given by:

$$P_{fail}(X) = \frac{1}{2} \operatorname{erfc} \left[\frac{27-3-18.9-X}{\sigma\sqrt{2}} \right] = \frac{1}{2} \operatorname{erfc} \left[\frac{5.1-X}{\sigma\sqrt{2}} \right] \quad (1)$$

where $\sigma=7.62\text{dB}$ (the standard deviation of the curve in Figure 10) and the function $\operatorname{erfc}(x)$ is the complementary error function.

The theoretical probability of failure given by Equation 1 is compared with the experimentally observed probability of failure in Figure 11, as a function of the source signal generator power $X\text{dBm}$. The experimental probability of failure in Figure 11 was determined by observing the number of positions of the stirrer at which the parking sensor was found to fail, as the stirrer was rotated through 360° , for each signal generator power considered. A total number of 177 independent positions for the stirrer were examined (approximately 2° steps) at each signal generator power, giving a resolution in Figure 11 of $1/177 \approx 0.00565$ in the experimental PDF. At the minimum signal generator power considered in Figure 11 (-10dBm), only 2 out of 177 stirrer positions resulted in a parking sensor failure. Clearly the experimental probability of failure below -10dBm signal generator power is not going to be very meaningful, and this imposes a lower limit on the abscissa in Figure 11.

V. CONCLUSION

This paper illustrates the potential for the use of reverberation chambers for testing systems that may be installed on vehicles and integrating the test results with a quantitative risk assessment of the vehicle operated in a real environment.

V. ACKNOWLEDGEMENT

The work described in this paper was funded by the EU SAFETEL programme.

REFERENCES

- [1] T. Konefal, J. F. Dawson, A. Denton, T. M. Benson, C. Christopoulos, A. C. Marvin, S. J. Porter and D. W. P. Thomas, *Electromagnetic coupling between wires inside a rectangular cavity using multiple-mode-analogous-transmission-line circuit theory*, IEEE Transactions on Electromagnetic Compatibility, Vol. 43, No. 3, pp 261-272, August 2001.
- [2] R. Holland and R. St. John, *Statistical response of EM-driven cables inside an overmoded enclosure*, IEEE Transactions on Electromagnetic Compatibility, Vol. 40, No. 4, pp 311-324, November 1998.
- [3] D. A. Hill, *Electromagnetic theory of reverberation chambers*, National Institute of Standards and Technology (NIST) Technical Note 1506, Technology Administration, US Department of Commerce, December 1998
- [4] J. F. Dawson, T. Konefal, M. P. Robinson, A. C. Marvin, S. J. Porter and L. C. Chirwa, *Field statistics in an enclosure with an aperture: effect of Q-factor and number of modes*, IEEE International Symposium on EMC, Chicago, IL, USA, vol. 1, August 2005, pp141-146
- [5] M.P. Robinson, J. Clegg and A.C. Marvin, *Radio frequency electromagnetic fields in large conducting enclosures: effects of apertures and human bodies on propagation and field-statistics*, IEEE Transactions on Electromagnetic Compatibility, Volume 48, No. 2, May. 2006, pp.520-530.
- [6] P. H. Lever, *Automotive electromagnetic susceptibility testing*, MPhil. Thesis, Department of Engineering, University of Warwick, June 1994